Research in Astron. Astrophys. **2012** Vol. **12** No. **12**, 1597–1602
http://www.raa-journal.org *http://www.iop.org/journals/raa*

***R**esearch in*
***A**stronomy and*
***A**strophysics*

LETTERS

Confirming the 115.5-day periodicity in the X-ray light curve of ULX NGC 5408 X-1*

Xu Han[1], Tao An[2,4], Jun-Yi Wang[3,1], Ji-Ming Lin[1], Ming-Jie Xie[1], Hai-Guang Xu[5], Xiao-Yu Hong[2,4] and Sandor Frey[6]

[1] Key Laboratory of Cognitive Radio & Information Processing, Ministry of Education, Guilin University of Electronic Technology, Guilin 541004, China; *wangjy@guet.edu.cn*
[2] Shanghai Astronomical Observatory, Chinese Academy of Sciences, Shanghai 200030, China; *antao@shao.ac.cn*
[3] School of Mathematics and Computational Science, Xiangtan University, Xiangtan 411105, China
[4] Key Laboratory of Radio Astronomy, Chinese Academy of Sciences, Nanjing 210008, China
[5] Department of Physics, Shanghai Jiao Tong University, Shanghai 200240, China
[6] FÖMI Satellite Geodetic Observatory, P.O. Box 585, H-1592 Budapest, Hungary

Received 2012 August 9; accepted 2012 October 4

Abstract The Swift/XRT light curve of the ultraluminous X-ray source NGC 5408 X-1 was re-analyzed with two new numerical approaches, the Weighted Wavelet Z-transform and CLEANest, and the results are different from previous studies. Both techniques detected a prominent periodicity with a time scale of 115.5 ± 1.5 days, in excellent agreement with the detection of the same periodicity first reported by Strohmayer . Monte Carlo simulations were employed to test the statisitical confidence of the 115.5-day periodicity, yielding a statistical significance of $> 99.98\%$ (or $> 3.8\sigma$). The robust detection of the 115.5-day quasi-periodic oscillations, if they are due to the orbital motion of the binary, would infer a mass of a few thousand $M_{\odot}$ for the central black hole, implying there is an intermediate-mass black hole in NGC 5408 X-1.

Key words: methods: statistical — galaxies: individual (NGC 5408) — stars: oscillations

1 INTRODUCTION

The presence of supermassive black holes (SMBHs, $10^6 - 10^9\,M_{\odot}$) in the hearts of active galactic nuclei (AGNs) and stellar-mass black holes (BH) ($\sim 10\,M_{\odot}$) as the evolutionary remnants of massive stars has been widely accepted and also confirmed by extensive observations with various techniques. However, the existence of intermediate-mass black holes (IMBHs, $10^2 - 10^4 M_{\odot}$) remains a puzzle. IMBHs are thought to be the seeds of the SMBHs, the masses of which are subsequently built up either through the accretion of gas, or through hierarchical BH mergers (reviewed by Volonteri 2010). Therefore, the discovery of IMBHs is important for understanding the dynamics

* Supported by the National Natural Science Foundation of China.

of stellar clusters, formation of SMBHs and production of gravitational waves (Miller & Colbert 2004).

The detection of a population of ultraluminous X-ray sources (ULXs, with X-ray luminosity exceeding 10^{39} erg s^{-1}) invokes an interpretation that they might be accretion-powered objects which harbor IMBHs (e.g. Colbert & Mushotzky 1999). However, the high X-ray luminosity may also result from relativistically beamed emission. In this regard, the central object is not necessary an IMBH (King et al. 2001), or the high X-ray luminosity may represent a super-Eddington accretion of stellar-mass BHs (Begelman 2002). Alternatively, some regular ULXs might represent an extension of low-mass X-ray binaries (LMXBs; Liu et al. 2006). Determination of the mass of ULXs is crucial to distinguish between these rival interpretations of the physical nature of ULXs. The canonical methods of measuring dynamical mass that rely on direct measurements of the binary motion of the companion are often frustrating because the companion is usually too dim to be detected. On the other hand, indirect methods that are based on the fit of an X-ray spectral energy distribution (e.g., Makishima et al. 2000) and X-ray timing observations (e.g., Kaaret et al. 2006) also place constraints on the mass of the BH.

NGC 5408 X-1 is one of the few ULXs showing variable X-ray flux (Soria et al. 2004). The source shows quasi-periodic oscillations (QPOs) around 10–40 mHz observed with the XMM-Newton (Strohmayer et al. 2007; Dheeraj & Strohmayer 2012). Strohmayer (2009) recently claimed to discover QPOs in NGC 5408 X-1 with $P = 115.5 \pm 4$ days from the Swift/XRT monitoring data. However, Kaaret & Feng (2009) analyzed the same data set (the only difference is that Strohmayer performed exposure map corrections on the light curve) but did not detect significant periodicity, although they did find a clue to the 115-day periodicity. In contrast to Galactic X-ray binaries whose characteristic variability period is of the order of days, the search for periodicity of $\sim$100 days in NGC 5408 X-1 requires a rather long time span of observations. Except for M82 X-1 (Kaaret & Feng 2007), there are few other ULXs that have been monitored for such a long period. The QPO of NGC 5408 X-1 is crucial for better constraining the physical nature of this ULX: if the 115.5-day periodicity is due to the orbital motion of the binary, that would provide evidence for an IMBH in NGC 5408 X-1 (Strohmayer & Mushotzky 2009). Both groups mainly relied on the periodicity analysis on the Lomb–Scargle (LS) periodogram (Lomb 1976; Scargle 1981). However, the statistical significance of periodicities detected with the LS technique is still a controversial issue. The LS periodogram introduces a traditional confidence limit based on an exponential distribution e^{-z} (z is the highest peak), which is actually not accurate enough for random signals. Therefore additional time series analysis techniques are necessary to verify the detected periodicity.

In this Letter, we shall re-analyze the light curve of NGC 5408 X-1 to check the 115.5-day periodicity using two other numerical techniques, the Weighted Wavelet Z-transform (WWZ) and CLEANest, which are more robust than the LS periodogram. The statistical significance of detected periodicities will also be evaluated with Monte Carlo simulations.

2 THE ALGORITHM

Traditional methods that are used to search for and identify periodic fluctuations in time series are based on the Fourier transform. A modified Fourier-based periodogram method is called the Date-Compensated Discrete Fourier Transform (DCDFT: Ferraz-Mello 1981), which models the observed data as a linear combination of three trial functions of constant $1(t)$, $\cos(\omega t)$, and $\sin(\omega t)$. Astronomical data are usually not evenly sampled. However, the Fourier transform of an unevenly spaced time series may often introduce a myriad of complications, which results in altering the peak frequency slightly and changing the amplitude greatly, and even generating strong fake peaks. In order to identify true periodic signals out of a time series containing multiple periodicities, an updated algorithm named CLEANest (Foster 1995) was developed. The CLEANest technique successively subtracts the strongest peaks in the original power spectrum detected by the DCDFT, until

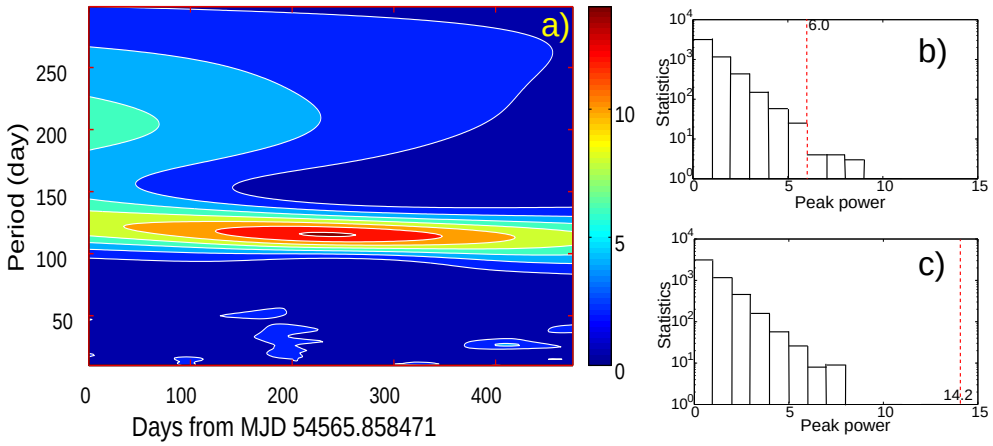

Fig. 1 WWZ periodogram of NGC 5408 X-1 (a) and the statistical histograms of Monte-Carlo simulations of the 210-day periodicity (b) and of the 115.5-day periodicity (c). The red dashed lines in (b) and (c) denote the peak powers of the periodic components in (a). To the right of the boundary line, the WWZ power of the simulated light curves is higher than the observed value; the ratio of the accumulated count of these light curves to the total test number (i.e., 5000) corresponds to the probability of the periodicity being induced by pure noise.

the strongest remaining peak in the residual spectrum is statistically not significant. These processes stop when the residual spectrum is relatively low and flat. The advantage of the CLEANest technique is that the significant frequencies involved would be refined at each iteration of the CLEANest procedure, thus the fake peaks induced by the sidelobe effect of the primary peaks are greatly reduced.

Compared to the Fourier analysis method that considers only frequency, the wavelet transform is remarkable for its property of localization in both time and frequency domains. The wavelet transform decomposes the signals into a combination of wavelet functions which can be scaled and shifted in time and frequency. The (quasi-)periodic behaviors of the signals can be identified through visual observations of the wavelet power as a function of transformation (time) and dilation (frequency), and the characteristic frequency (or time scale) is determined by looking for peaks in the time-averaged wavelet power (Grossmann et al. 1989). For unevenly-sampled data, the fluctuations of the local number density may induce spurious high-frequency spikes and also result in fake time evolution behavior of the characteristic periods. In order to resolve these problems, Foster (1996) proposed a rescaled wavelet method called WWZ. Like the canonical wavelet transforms, WWZ is also a kind of projection for functions which projects the signals onto three trial functions: a constant function $\varphi_1(t) = 1(t)$, $\varphi_2(t) = \cos(\omega(t-\tau))$, and $\varphi_3(t) = \sin(\omega(t-\tau))$, where ω is the dilation parameter, also called the scale factor, and τ is the time shift. The difference is that WWZ adopts statistical weights $\omega_a = \exp[-c\omega^2(t_\alpha - \tau)^2]$ (α=1, 2, 3) for the projection on the trial functions, where the constant c determines how rapidly the wavelet decays. The WWZ power is defined as Z-statistics, $WWZ = (N_{\rm eff} - 3)/2(V_x - V_y)$ (Foster 1996), where $N_{\rm eff}$ is the effective number of data points, which represents the statistical data density, and V_x and V_y are the weighted variation of the data and the weighted variation of the model function, respectively. In doing so, WWZ follows an F-distribution with $N_{\rm eff} - 3$ and 2 degrees of freedom. The CLEANest and WWZ techniques have been widely used in studies of variable stars (e.g., Kiss et al. 1999; Templeton 2004). Recently, they have also been successfully applied to X-ray timing analysis of AGNs and X-ray binaries (e.g., Espaillat et al. 2008; Lachowicz et al. 2006).

3 RESULTS

Results of the periodicity analysis derived from WWZ are presented in Figure 1. The power of WWZ is shown as a function of both observing time (x-axis) and testing period (y-axis) (Fig. 1(a)). The peaks in the WWZ power indicate the strength and duration of a characteristic periodicity. The majority of the WWZ power is dominated by the most prominent component whose peak marks a characteristic period of 115.5 days, and this periodic component spreads across the whole time span with a scattering of ± 1.5 days. The amplitude of the 115.5-day component is 14.2, significantly higher than the secondary peak of 6.0, which corresponds to a characteristic period of $\sim$210 days. The ridge line of the contours of the 210-day periodic component shows a large variation from 184 to 226 days.

Figure 2 shows the power spectra made from the Fourier transform analysis: the DCDFT (Fig. 2(a)) and CLEANest (Fig. 2(b)). In the DCDFT spectrum (Fig. 2(a)), there are two peaks higher than half of the maximal amplitude. The primary peak is located at a characteristic frequency of 0.00866 day^{-1}, corresponding to a period of 115.5 days. The secondary peak falls in a relatively broad range from 194 to 236 days; the highest peak denotes a period of $\sim$210 days.

The periodograms derived from WWZ and DCDFT show excellent consistency, and they are also in agreement with previous results based on the LS periodogram analysis (Strohmayer 2009) showing a distinct primary peak at a period of 115.5 days, and a scattered secondary at a period of $\sim$210 days. Note Strohmayer (2009) also detected the secondary peak at P2$\sim$210 days in his figure 2, although the author did not remark on the secondary. The harmonic relation between two characteristic periods (frequency ratio $\sim$2:1) and the scattered appearance of the secondary are reminiscent that the 210-day periodicity might be an artifact due to the sidelobe of the primary. Therefore we further run the CLEANest algorithm to check the reliability of the secondary periodic component. After subtracting the strongest 115.5-day peak, the residual CLEANest spectrum shown in Figure 2(b) becomes rather flat, and no longer shows any significant peak. That gives evidence that the 210-day peak detected in the WWZ and DCDFT spectrum is probably a fake signal which is contaminated by the nearby primary component with a period of 115.5 days.

In order to further constrain the nature of the periodicities detected by the WWZ, we performed statistical confidence tests with Monte Carlo simulations (Linnell Nemec & Nemec 1985). First we created a series of 5000 light curves with added noise following a Poisson distribution to represent the random observational errors. The simulated light curves had the same number of sampled data points (113), temporal baseline (485 days), mean sampling rate ($\sim$14 days) and error variance as the observed light curve. The observed data were randomized in this way. We then calculated the WWZ periodograms for each of the simulated light curves using the same parameters as for the observed light curve. Next in the frequency channel corresponding to the 115.5-day periodicity, we searched for the periodograms in which the peak power exceeded 14.2, i.e., the peak power of the 115.5-day periodicity, and counted the number of the light curves. This accumulated number represents the number of times that the 115.5-day periodicity could be generated by pure noise. The ratio of this number to the total number of tests denotes a probability of false detection for the periodicity due to noise in the observed light curve. The 210-day periodicity was tested following the same procedure. The histograms of the Monte Carlo simulations are displayed in Figure 1(b) (210 days) and 1(c) (115.5 days).

In Figure 1(c), most of the power of the simulated light curves is lower than 8.0, with only two exceptions higher than 10.0 but lower than 14.2 (the peak power derived from the observed data), placing a lower limit on the confidence level of 99.98% (or $> 3.8\sigma$). Compared with the observed WWZ periodogram in Figure 1(a), the simulations provide unambiguous evidence for the detection of the 115.5-day periodicity across the whole observed period. In Figure 1(b), there are 13 simulated light curves that may generate peak powers of the 210-day periodicity higher than that from the observed data, setting an upper limit on the statistical confidence of 99.74% ($\lesssim 3\sigma$).

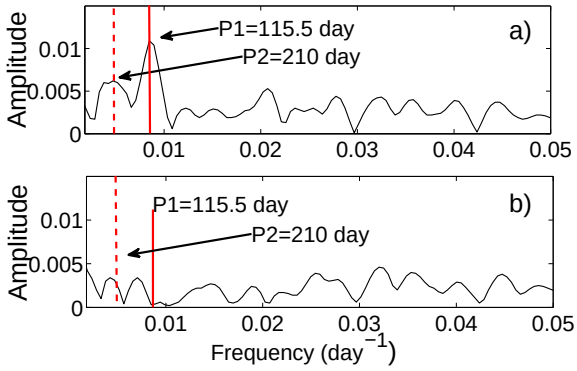

Fig. 2 The DCDFT (*top*) and CLEANest (*bottom*) periodograms of NGC 5408 X-1. The vertical solid line indicates the 115.5-day periodic component. The vertical dashed line indicates the fake 210-day period.

4 DISCUSSION

In the present work, two numerical techniques, WWZ and CLEANest, were used to search for periodicities in the Swift/XRT light curve of NGC 5408 X-1. Both WWZ and DCDFT periodograms detected a distinct component across the whole time span corresponding to a 115.5-day period, which is in good agreement with previous work (Strohmayer 2009). Monte Carlo simulations were employed to test the statistical significance of the 115.5-day periodicity. The simulations indicate a high confidence level of $>$99.98%, excluding the possibility that the periodicity is generated by random noise. All the evidence points to a conclusion that the X-ray light curve of NGC 5248 X-1 intrinsically displays QPOs with a time scale of 115.5 days.

A straightforward interpretation of the 115.5-day periodicity is the orbital period of the binary system, resembling QPOs detected in Galactic BH binaries such as XTE J1550–564 and GRS 1915+105 (Strohmayer 2009 and references therein). The difference between NGC 5408 X-1 and the Galactic BH binaries is that the time scale in NGC 5408 X-1 is longer by a factor $\sim$100, implying a larger dynamic mass for the central BH. If the low-frequency QPO in NGC 5408 X-1 is analogous to Galactic BH binaries in terms of its physical nature, the mass of the NGC 5408 X-1 BH might be estimated from the Galactic BH mass and the scaling factor of the QPO frequencies. This gives an estimated mass of the NGC 5408 X-1 BH ranging from 1000 $M_{\odot}$ to 9000 $M_{\odot}$ (Strohmayer & Mushotzky 2009).

In addition to the scenario involving orbital motion, there are other arguments for this QPO in NGC 5408 X-1. Foster et al. (2010) claimed that the 115.5-day QPO is probably a manifestion of jet precession resembling SS 433, and is thus superorbital in nature. Therefore NGC 5408 X-1 might in fact be a large stellar-mass BH accreting with a super-Eddington rate to account for the high X-ray luminosity (Middleton et al. 2011). Similarly, Soria (2007) proposed that the accretion properties of ULXs are different from stellar-mass BHs, and low-frequency milli-Hz QPOs cannot be used as an indicator of high BH mass. In their model, the ULXs can be 50–100 $M_{\odot}$-mass BHs with a high accretion rate.

Continuing observations of X-ray timing and studies of energy spectra are necessary to discriminate between the different scenarios for explaining the 115.5-day periodicity. If further observations can confirm that the 115.5-day periodicity is indeed related to the orbital motion of the binary system, NGC 5408 X-1 would be one of the few IMBH candidates in an extragalactic system.

Acknowledgements The authors thank the anonymous referee for a quick response and helpful comments. This work is partly supported by the National Basic Research Program of China (973 Program, Grant Nos. 2009CB24900 and 2013CB837901), the National Natural Science Foundation of China (Grant No. 61261017), the Strategic Priority Research Program of the CAS (XDA04060700), the China-Hungary Exchange Program of the CAS, the Hungarian Scientific Research Fund (OTKA K104529) and the Science & Technology Commission of Shanghai Municipality (06DZ22101).

References

Begelman, M. C. 2002, ApJ, 568, L97
Colbert, E. J. M., & Mushotzky, R. F. 1999, ApJ, 519, 89
Dheeraj, P. R., & Strohmayer, T. E. 2012, ApJ, 753, 139
Espaillat, C., Bregman, J., Hughes, P., & Lloyd-Davies, E. 2008, ApJ, 679, 182
Ferraz-Mello, S. 1981, AJ, 86, 619
Foster, G. 1995, AJ, 109, 1889
Foster, G. 1996, AJ, 112, 1709
Foster, D. L., Charles, P. A., & Holley-Bockelmann, K. 2010, ApJ, 725, 2480
Grossmann, A., Kronland-Martinet, R., & Morlet, J. 1989, in Wavelets. Time-Frequency Methods and Phase Space, eds. J.-M. Combes, A. Grossmann, & P. Tchamitchian (Berlin: Spinger), 2
Kaaret, P., & Feng, H. 2007, ApJ, 669, 106
Kaaret, P., & Feng, H. 2009, ApJ, 702, 1679
Kaaret, P., Simet, M. G., & Lang, C. C. 2006, ApJ, 646, 174
King, A. R., Davies, M. B., Ward, M. J., Fabbiano, G., & Elvis, M. 2001, ApJ, 552, L109
Kiss, L. L., Szatmáry, K., Cadmus, R. R., Jr., & Mattei, J. A. 1999, A&A, 346, 542
Lachowicz, P., Zdziarski, A. A., Schwarzenberg-Czerny, A., Pooley, G. G., & Kitamoto, S. 2006, MNRAS, 368, 1025
Linnell Nemec, A. F., & Nemec, J. M. 1985, AJ, 90, 2317
Liu, J.-F., Bregman, J. N., & Irwin, J. 2006, ApJ, 642, 171
Lomb, N. R. 1976, Ap&SS, 39, 447
Makishima, K., Kubota, A., Mizuno, T., et al. 2000, ApJ, 535, 632
Middleton, M. J., Roberts, T. P., Done, C., & Jackson, F. E. 2011, MNRAS, 411, 644
Miller, M. C., & Colbert, E. J. M. 2004, International Journal of Modern Physics D, 13, 1
Scargle, J. D. 1981, ApJS, 45, 1
Soria, R. 2007, Ap&SS, 311, 213
Soria, R., Motch, C., Read, A. M., & Stevens, I. R. 2004, A&A, 423, 955
Strohmayer, T. E., Mushotzky, R. F., Winter, L., et al. 2007, ApJ, 660, 580
Strohmayer, T. E. 2009, ApJ, 706, L210
Strohmayer, T. E., & Mushotzky, R. F. 2009, ApJ, 703, 1386
Templeton, M. 2004, Journal of the American Association of Variable Star Observers (JAAVSO), 32, 41
Volonteri, M. 2010, A&A Rev., 18, 279